Nuclear Inst. and Methods in Physics Research, A 909 (2018) 160–163

Contents lists available at ScienceDirect

Nuclear Inst. and Methods in Physics Research, A

journal homepage: www.elsevier.com/locate/nima

Light Ion Accelerating Line (L3IA): Test experiment at ILIL-PW

L.A. Gizzi [a,b,*], F. Baffigi [a], F. Brandi [a], G. Bussolino [a,b], G. Cristoforetti [a], A. Fazzi [c], L. Fulgentini [a], D. Giove [d], P. Koester [a], L. Labate [a,b], G. Maero [e], D. Palla [a], M. Romé [e], P. Tomassini [a]

[a] Intense Laser Irradiation Laboratory, INO-CNR, Pisa, Italy
[b] INFN, Sez. Pisa, Italy
[c] Dipartimento di Energia, Politecnico di Milano and INFN, Sezione di Milano, Italy
[d] INFN-LASA, Segrate, Italy
[e] Università di Milano and INFN Sez. Milano, Italy

ARTICLE INFO

Keywords:
Ultraintense lasers
Laser–plasma acceleration
Target normal sheath acceleration
Ion detection

ABSTRACT

The construction of a novel Laser-driven Light Ions Acceleration Line (L3IA) is progressing rapidly towards the operation, following the recent upgrade of the ILIL-PW laser facility. The Line was designed on the basis of the pilot experimental activity carried out earlier at the same facility to define design parameters and to identify main components including target control and diagnostic equipment, also in combination with the numerical simulations for the optimization of laser and target parameters. A preliminary set of data was acquired following the successful commissioning of the laser system > 100 TW upgrade. Data include output from a range of different ion detectors and optical diagnostics installed for qualification of the laser–target interaction. An overview of the results is given along with a description of the relevant upgraded laser facility and features.

1. Introduction

Novel acceleration techniques based on ultraintense lasers are evolving rapidly from scientific exploration to applications, relying on established and extensively investigated [1] acceleration processes like the Target Normal Sheath Acceleration (TNSA) [2].

Examples of applications include injectors for high power ion beams, neutron generation [3], probes for fast evolving phenomena like the ultrafast charging of laser-heated samples [4], space radiation studies and electronic components testing [5]. Applications with potential impact on industry and cultural heritage like the proton-induced X-ray emission spectroscopy (PIXE) may be applicable with currently achievable TNSA performances and may strongly benefit from the compactness of a multi-MeV laser-driven ion source [6].

Laser-based applications requiring multi MeV ions are being developed for industrial use, in view of the ongoing evolution of the next generation of Joule-scale laser drivers in the sub-100 fs domain, which may become attractive [7] for their higher repetition rate, potentially reaching the 100 Hz or even the kHz range. In fact, with the ongoing transition to an extensive use of diode-pumping in high power lasers [8], high repetition rate and higher efficiency TNSA drivers may soon be available enabling laser-driven high average power sources to become finally commercially available.

At the same time, great attention is being dedicated to the control of acceleration parameters to enhance TNSA performances, including energy cut-off, beam divergence, charge, emittance. Target optimization and engineering, looking at different properties of surface, geometry and conductivity are becoming crucial in this effort, with nano-structured targets emerging as a potential breakthrough in table-top laser-driven ion sources development [9]. Finally, post acceleration is being tackled with special attention to selection, collimation [10] and injection in secondary acceleration structures, even using miniature target-driven guiding devices [11].

Here we describe the preliminary results of the commissioning experiment of a new Line for Laser-driven Light Ions Acceleration (L3IA) with the purpose of establishing an outstanding beam-line operation of a laser–plasma source in Italy taking advantage of the results achieved so far in this field by the precursor activity [12] and based upon experimental campaigns and numerical modeling. The beam-line will operate in the parameter range of ion acceleration currently being explored by leading European laboratories in this field and will provide an advanced test facility for the development of laser-driven ion sources.

* Corresponding author at: Intense Laser Irradiation Laboratory, INO-CNR, Pisa, Italy.
E-mail address: la.gizzi@ino.cnr.it (L.A. Gizzi).

https://doi.org/10.1016/j.nima.2018.03.016
Received 8 December 2017; Received in revised form 14 February 2018; Accepted 7 March 2018
Available online 27 March 2018

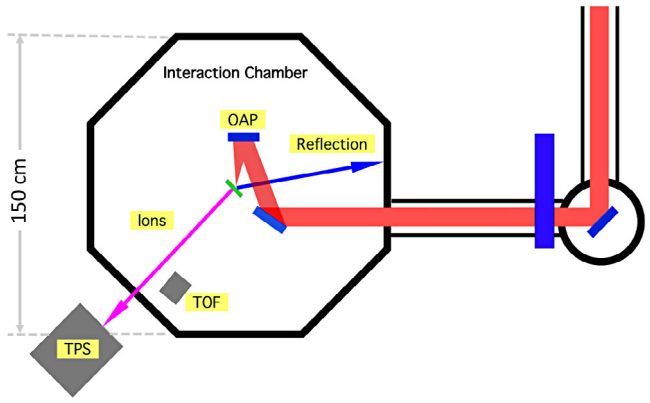

Fig. 1. Schematic experimental setup showing the octagonal target chamber, the off-axis parabola and the main diagnostics.

The project includes a complete set of work-packages, including the interface with the ILIL-PW facility, the beam line scheme comprising targets, laser beam focusing, and diagnostic devices dedicated to both the laser–plasma interaction and the ion beam detection and characterization. Numerical modeling is also included, with the specific tasks of providing basic predictive simulations for the baseline parameters of the beam line and also allowing investigation of advanced target and laser configurations. Provision is also made for specific application cases, including radiobiological testing and cultural heritage applications.

2. Experimental set up

The experiment was carried out at the Intense Laser Irradiation Laboratory using the ILIL-PW Ti:Sa laser and interaction facility with laser pulse parameters related to the phase 1 configuration described in Ref. [13]. Preliminary results obtained using the laser pulse at the output of the front-end can be found in Ref. [13]. In the same reference, an overview of the ILIL-PW facility and a summary of the main laser parameters are also presented. In the experiment presented here the pulse duration was 30 fs and the pulse energy was 3 J on target.

A schematic view of the experimental set up is given in Fig. 1. The 100 mm diameter laser beam was focused by an F/4.5 Off-Axis Parabolic (OAP) mirror with an angle of incidence of 15°. The focal spot was elliptical, with an average diameter of 4.4 μm (FWHM) and an intensity in excess of 1.6×10^{20} W/cm^2 ($a_0 = 8.6$). The target was mounted in a remotely controlled motorized support with a sub-micrometer resolution, capable of XYZ translation and azimuthal rotation around the vertical axis.

As shown in Fig. 2, the target mount consisted of a solid steel frame machined to leave access to the surface of the foil from both sides through a set of 500 μm diameter holes with conical aperture to allow oblique laser incidence on target. The whole mount was designed to enable a 100-mm range of positioning and withstand a load of up to 500 N in all directions of motion. These specifications ensure that the scanning of targets up to 100 mm × 100 mm can be accomplished, enabling a large number of laser shots to be fired on a given target before target replacement is required. In the measurements discussed here the target consist of a 10 μm Al foil.

Special attention was dedicated, during the experiment, to establish target integrity at the time of arrival of the main pulse on target which strongly depends on the temporal profile of the laser pulse [14]. A cross-correlation curve of the laser pulse taken with the Sequoia (Amplitude Technologies) is shown in Fig. 3. According to this plot, the laser contrast is greater than 10^7 up to 10 ps before the peak of the pulse. A detailed modeling of laser–target interaction with such a laser temporal profile is in progress, but we can anticipate that with the measured laser

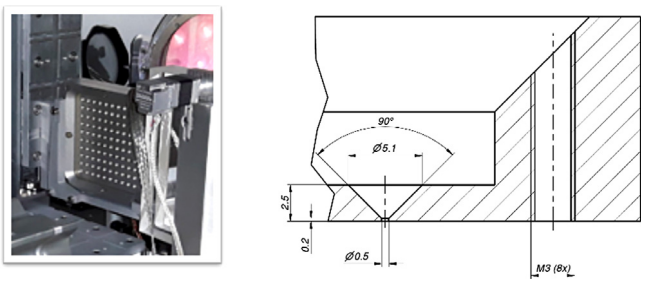

Fig. 2. (left) Target mount showing the 500 μm hole array. (right) Detail showing the conical hole geometry.

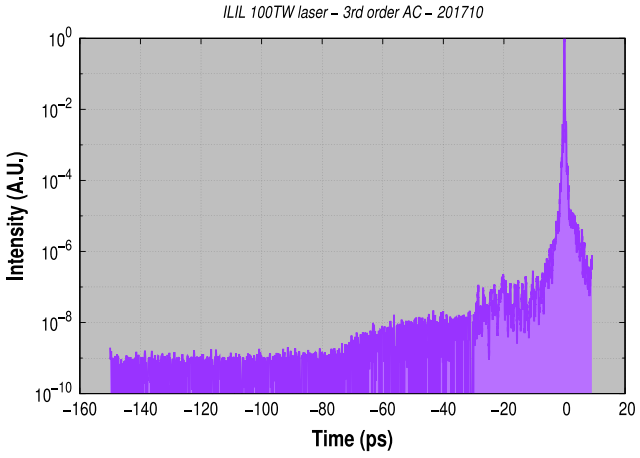

Fig. 3. Cross-correlation curve of the laser pulse.

contrast, no major pre-plasma formation occurs, ensuring bulk target survival at the peak of the pulse.

These circumstances were further confirmed by optical spectroscopy of the light scattered in the specular direction, collected shot by shot using a F/5 collecting lens placed in vacuum to collimate scattered light outside the target chamber. Light was than attenuated using neutral filters and rejecting filters at 800 nm and focused on the tip of a fiber coupled to a spectrometer. This set up enabled detection of second harmonic emission, $2\omega_L$, and $(3/2)\,\omega_L$ of the incident laser light scattered in the specular direction. Such components are associated to the coupling of the laser light at the critical density and at the quarter critical density respectively [15].

In fact, the formation of even a very small pre-plasma before of the arrival of the main pulse can provide suitable conditions for the growth of stimulated instabilities including the Stimulated Raman Scattering and the Two Plasmon Decay (see [6] and references therein). Electron plasma waves at $\omega_L/2$ generated by the instabilities can couple non-linearly with the incident laser light and give rise to $(3/2)\,\omega_L$ emission. This emission is therefore a signature of the presence of even a small pre-plasma.

Second harmonic emission in the specular direction is generated by the non-linear interaction of the main laser pulse at the critical density [16]. Therefore, second harmonic emission can be taken as a signature of the presence of a critical density layer in the plasma at the time of interaction of the main pulse, a prerequisite for the interaction with an over-dense target and the occurrence of TNSA.

As shown by Fig. 4, in our experiments, in spite of the increase of the $(3/2)\,\omega_L$ intensity compared to the previous experimental campaign at 10 TW [13], the intensity of the $2\omega_L$ emission remains always significant, indicating that the laser contrast in the best focus is sufficient to ensure survival of an overdense target.

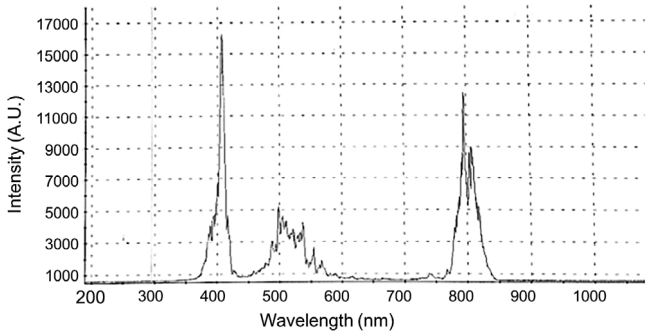

Fig. 4. A typical spectrum obtained with the target placed near the best focus. The second harmonic component at 400 nm is used to monitor the survival of the target at the peak of the pulse.

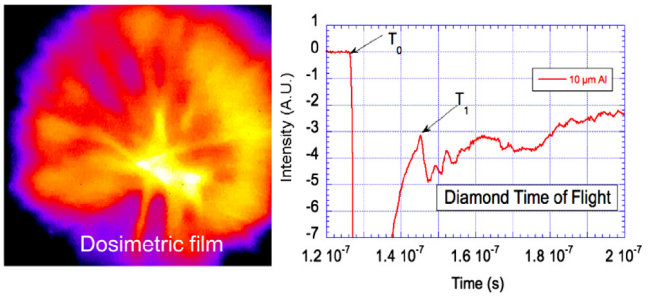

Fig. 5. (left) The signal from the GAFchromic™ EBT-3 film placed at 100 mm from the target rear surface. (right) Signal of the diamond Time of Flight (TOF) showing the ion signal from the irradiation of a 10 μm thick aluminium target. $T = 0$ is arbitrary in this plot. The strong emission in the range $t = [T_0 - T_1]$ is the signal due to fast electrons. For $t > T_1$ the signal is due to ions detection.

3. Results and discussion

A range of diagnostics were used in our experiments to measure ion acceleration, including radio-chromic films (GAF), CR39, Thomson Parabola, and Time of Flight (TOF) diamond detectors. Thomson Parabola Spectrometer (TPS) and a TOF detector were used simultaneously so that a cross-comparison of the signals obtained from the two devices was possible. This was done in view of a possible use of the diamond detector for on-line direct detection of accelerated ions during normal operation. A detailed discussion of all these measurements with different detectors is given elsewhere [17,18]. Here, we focus our attention on the presentation of the preliminary results of TOF and TPS signals obtained during the currently operating L3IA phase 1 configuration.

A typical GAF image obtained with a 10 μm thick Al target is shown in Fig. 5(left), showing an intense on-axis spot, surrounded by a broader signal.

Fig. 5(right) shows the plot of the TOF signal obtained with the diamond detector from the irradiation of the same 10 μm thick Al target. The TOF detector was placed at a distance of 60 cm from the target rear side and was filtered using a 12 μm thick Al foil. The strong peak between $t = T_0$ and $t = T_1$ is attributed to a combination of X-rays and fast electrons reaching the detector soon after the interaction [13,17]. This peak is then followed by the actual ion signal that starts at $t = T_1$. Taking into account the TOF distance and assuming a signal predominantly due to protons that have the highest charge-to-mass ratio, calculations yield a high energy cut-off of approximately 5 MeV.

For the same aluminium shot, the raw TPS spectrogram is also presented in Fig. 6, showing the parabolic traces of protons and carbons with different ionization states. As we can see, the assumption that the TOF ion signal is predominantly due to protons is consistent with

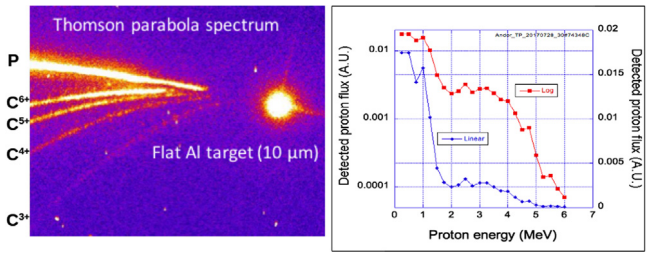

Fig. 6. Image of the Thomson Parabola Spectrometer (TPS) spectrogram from a 10-μm thick aluminium target showing protons and carbon ions with different charge states. The proton spectrum is also reported (right) in logarithmic scale showing the proton cut-off energy of 6 MeV.

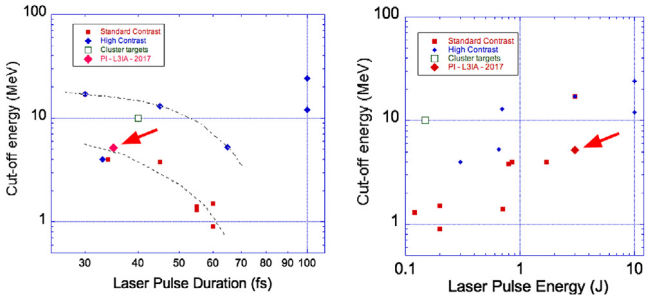

Fig. 7. Summary of data from published TNSA experiments (after [1]) showing measured dependence upon laser pulse duration (left) and laser pulse energy (right). The arrows indicate the cutoff energy of our experiment.

the TPS signal showing a bright proton signal. The analysis of the TPS proton spectrum is presented in Fig. 6(right). The measured proton cut-off energy considering the minimum detectable signal above noise is 6 MeV. The TPS measurement is in agreement with the TOF estimate that is done at a higher signal level. The possibility of using our TOF detector for a reliable, online shot to shot proton energy evaluation is therefore confirmed.

It is interesting to compare the measured cut-off energy with published results obtained in similar interaction conditions. A summary of published results relevant for our experimental conditions, taken from [1], is displayed in Fig. 7 as a function of laser pulse duration (left) and laser pulse energy (right) showing the cut-off of our experiment for comparison. These plots show that the cut-off energy measured in our experiment is in agreement or even exceeds the cut-off values measured in similar experiments with standard contrast (no plasma mirror).

Our preliminary results from this commissioning experiment meet the expectations from first phase of L3IA as anticipated [13], enabling foreseen applications. Further increase of ion energy and flux will require fine tuning of laser pulse parameters and target optimization.

4. Conclusions

In summary, we described the preliminary data obtained during an experiment dedicated to the commissioning of the new laser-driven light ions acceleration line (L3IA). Our experiment shows proton acceleration cut-off energies up to 6 MeV which are in a perfect agreement with intensity scaling established by previous measurements in similar interaction conditions. Our data demonstrate overall laser and target performances of our setup in line with project specification planned for Phase 1.

Acknowledgments

This project has received funding from the CNR funded Italian research Network ELI-Italy (D.M. n.631 08.08.2016) and from the L3IA

INFN Experiment of CSN5. We gratefully acknowledge support from the Central Laser Facility for in kind contribution to the experimental set up described in this experiment.

References

[1] H. Daido, M. Nishiuchi, A.S. Pirozhkov, Review of laser-driven ion sources and their applications, Rep. Progr. Phys. 75 (2012) 056401.
[2] R.A. Snavely, Intense high-energy proton beams from petawatt-laser irradiation of solids, Phys. Rev. Lett. 85 (2000) 2945–2948.
[3] M. Roth, M. Schollmeier, Ion acceleration — target normal sheath acceleration, in: Proceedings of the CERN Conference, Geneva, Switzerland, 23–29 November 2014, C14-11-23, pp. 231–270, http://dx.doi.org/10.5170/CERN-2016-001.231.
[4] H. Ahmed, S. Kar, G. Cantono, G. Nersisyan, S. Brauckmann, D. Doria, D. Gwynne, A. Macchi, K. Naughton, O. Willi, et al., Investigations of ultrafast charge dynamics in laser-irradiated targets by a self probing technique employing laser driven protons, Nucl. Instrum. Methods Phys. Res. A 829 (2016) 172–175.
[5] B. Hidding, T. Königstein, O. Willi, J. Rosenzweig, K. Nakajima, G. Pretzler, et al., Laser–plasma- accelerators — A novel, versatile tool for space radiation studies, Nucl. Instrum. Methods Phys. Res. A 636 (2011) 31–40.
[6] M. Barberio, S. Veltri, M. Scisciò, P. Antici, Laser-accelerated proton beams as diagnostics for cultural heritage, Sci. Rep. 7 (2017) 40415.
[7] M. Noaman-ul Haq, H. Ahmed, T. Sokollik, L. Yu, Z. Liu, X. Yuan, F. Yuan, M. Mirzaie, X. Ge, L. Chen, et al., Statistical analysis of laser driven protons using a high-repetition-rate tape drive target system, Phys. Rev. Accel. Beams 20 (2017) 041301.
[8] P. Mason, M. Divoky, K. Ertel, J. Pilar, T. Butcher, M. Hanus, S. Banerjee, J. Phillips, J. Smith, M. De Vido, et al., Kilowatt average power 100 J-level diode pumped solid state laser, Optica 4 (2017) 438–439.
[9] M. Blanco, M.T. Flores-Arias, C. Ruiz, M. Vranic, Table-top laser-based proton acceleration in nanostructured targets, New J. Phys. 19 (3) (2017) 033004.
[10] F. Romano, F. Schillaci, G.A.P. Cirrone, G. Cuttone, V. Scuderi, L. Allegra, A. Amato, A. Amico, G. Candiano, G.D. Luc, et al., The ELIMED transport and dosimetry beamline for laser-driven ion beams, Nucl. Instrum. Methods Phys. Res. A 829 (2016) 153–158.
[11] S. Kar, H. Ahmed, R. Prasad, M. Cerchez, S. Brauckmann, B. Aurand, G. Cantono, P. Hadjisolomou, C.L.S. Lewis, A. Macchi, G. Nersisyan, A.P.L. Robinson, A.M. Schroer, M. Swantusch, et al., Guided post-acceleration of laser-driven ions by a miniature modular structure, Nature Commun. 7 (2016) 10792.
[12] S. Agosteo, M.P. Anania, M. Caresana, G.A.P. Cirrone, C. de Martinis, D.D. Side, A. Fazzi, G. Gatti, D. Giove, D. Giulietti, et al., The LILIA (laser induced light ions acceleration) experiment at LNF, Nucl. Instrum. Methods Phys. Res. B 331 (2014) 15–19.
[13] L.A. Gizzi, D. Giove, C. Altana, F. Brandi, P. Cirrone, G. Cristoforetti, A. Fazzi, P. Ferrara, L. Fulgentini, P. Koester, L. Labate, G. Lanzalone, P. Londrillo, D. Mascali, A. Muoio, D. Palla, F. Schillaci, S. Sinigardi, S. Tudisco, G. Turchettie, A new line for laser-driven light ions acceleration and related TNSA studies, Appl. Sci. 7 (2017) 984.
[14] F. Baffigi, G. Cristoforetti, L. Fulgentini, A. Giulietti, P. Koester, L. Labate, L.A. Gizzi, X-ray conversion of ultra- short laser pulses on a solid sample: Role of electron waves excited in the pre- plasma, Phys. Plasmas 21 (2014) 072108.
[15] L.A. Gizzi, in: K. Yamanouchi, A. Giulietti, K. Ledingham (Eds.), Advances in X-ray Studies of Ultraintense Laser–Plasma Interactions, in: Progress in Ultrafast Intense Laser Science, vol. 98, Springer, New York, NY, USA, 2010, pp. 123–138.
[16] L.A. Gizzi, D. Giulietti, A. Giulietti, P. Audebert, S. Bastiani, J.P. Geindre, A. Mysyrowicz, Simultaneous measurements of hard X-rays and second-harmonic emission in fs laser-target interactions, Phys. Rev. Lett. 76 (1996) 2278.
[17] L.A. Gizzi, C. Altana, F. Brandi, P. Cirrone, G. Cristoforetti, A. Fazzi, P. Ferrara, L. Fulgentini, D. Giove, P. Koester, et al., Role of laser contrast and foil thickness in target normal sheath acceleration, Nucl. Instrum. Methods Phys. Res. A 829 (2016) 144–148.
[18] C. Altana, A. Muoio, G. Lanzalone, S. Tudisco, F. Brandi, G.A.P. Cirrone, G. Cristoforetti, A. Fazzi, P. Ferrara, L. Fulgentini, et al., Investigation of ion acceleration mechanism through laser-matter interaction in femtosecond domain, Nucl. Instrum. Methods Phys. Res. A 829 (2016) 159–162.